Ecohydrology & Hydrobiology xxx (xxxx) xxx

Contents lists available at ScienceDirect

Ecohydrology & Hydrobiology

journal homepage: www.elsevier.com/locate/ecohyd

Original Research Article

Evaluation of perennial reference evapotranspiration (ET_o) over a typical dryland using satellite images: a case study from Uzbekistan

Umida Makhmudova[a], Sayidjakhon Khasanov[b,c,d,*], Akmal Karimov[a], Sarvar Abdurakhmonov[a]

[a] *"Tashkent Institute of Irrigation and Agricultural Mechanization Engineers" National Research University, Tashkent, 100000, Uzbekistan*
[b] *Institute of Geographic Sciences and Natural Resources Research, Chinese Academy of Sciences, Beijing, 100101, China*
[c] *University of Chinese Academy of Sciences, Beijing, 101408, China*
[d] *Research Institute of Environment and Nature Conservation Technologies, Tashkent, 100043, Uzbekistan*

ARTICLE INFO

Article history:
Received 1 June 2022
Revised 27 December 2022
Accepted 12 March 2023
Available online xxx

Keywords:
Air temperature
solar irradiance
leaf area index
land cover change
evapotranspiration
agricultural land
Hargreaves-Samani
NDVI
SAVI
climate change
Karakalpakstan

ABSTRACT

Evapotranspiration (ET) is one of the most significant compartments in the energy and water balance between the atmosphere and the Earth's surface. Global climate change has an impact on the water cycle and can result in an increase in ET from the land surface; nevertheless, an increase in ET can destabilize the macro- and micro-climate at the local and continental levels. In line with this, the purpose of this article is to learn more about the factors that contribute to the high and current reference ET (ET_o) rate of Karakalpakstan (Uzbekistan). MODIS Terra images was used to analyze long-term land cover change. The Google Earth Engine code editor, Erdas Imagine 2020, and ArcMap 10.8 were used to map land cover change and the leaf area index (LAI). Though the Normalized Difference Vegetation Index and the Soil-Adjusted Vegetation Index were used because of their past performance as affirmative measurement techniques for vegetation monitoring. The Hargreaves-Samani equation was utilized to ET_o in this study. Increased crop density in agriculture and the conversion of barren soil to grasslands to rehabilitate the seashore ecosystem of the Aral Sea influenced LAI significantly, according to multifactorial analyses of perennial air temperature, land cover change, solar irradiance, and ET_o in a typical dryland of Uzbekistan. However, the extension of LAI in the agricultural area of Karakalpakstan substantially accelerated the ET_o rate, which was a key contributor of an increase in crop water demand. We can see that measured solar radiation and ET_o were consistent across time by looking at the nearly same quantities for both. As a result, we assume that global climatic changes have no effect in the uncertainty of solar radiation and ET rate.

1. Introduction

Evapotranspiration (hereinafter, ET) is deemed as one of the important compartments in the energy and water balance between atmosphere and Earth surface. ET is a process that occurs when energy and water are exchanged between soil, atmosphere, and vegetation, and interacts with climatic factors (Wang et al., 2019). Global climate variations influences the process of water cycle and can beget an increased ET rate from land surface (Vörösmarty et al., 2000), simultaneously an increased ET can also destabilize the macro- and micro-climate at local and continental levels (Pan et al., 2015; Shukla & Mintz, 1982).

* Corresponding author.
E-mail address: skhasanov@igsnrr.ac.cn (S. Khasanov).

https://doi.org/10.1016/j.ecohyd.2023.03.006
1642-3593/

Land cover change (hereinafter, LCC) has been captivating wide-scale attention over the decades since it induces ET change (Wang et al., 2021). Remote sensing based or spatial modelling investigations have revealed that the rehabilitation of forest resources can positively influence ET in humid areas (Jin et al., 2017), permanent shrublands (Gibson et al., 2018), whereas the deterioration of forest resources can lead to a decrease in ET in Amazonia rainforest (Hahmann & Dickinson, 1997). Nevertheless, the general consensus lied behind that the extension of canopy cover will increase the ET rate as a consequence of having deeper tree roots and consuming increased soil moisture (Adane et al., 2018; Sheil, 2018; Zhang et al., 2001). Two methodological aspects have remained ET induced by LCC at regional and global levels uncertain: insufficient perennial consistent and continuous observations of historical LCC and restricted investigations on diverse hydrological effects of LCC characteristics (Cornelissen et al., 2013; Lawrence et al., 2016; Peel et al., 2010; Pielke et al., 2011; Sheil, 2018). In line with a swift accumulation of canopy cover data throughout recent decades by remote sensing (Song et al., 2018), the potential impacts of LCC on regional and global ET using satellite data are now assessable, however, these types of investigations have rarely been undertaken at a regional or global level. Vast majority of the historical LCC impacts on a regional or global ET has enabled numerous scientists to obtain several scenarios of LCC based on discrete and fully constructed land use-land cover (LULC) maps (Gordon et al., 2005; Sterling & Ducharne, 2008). But, scientists have reported reasonable biases in these LULC maps. These scientific biases are emanated from non-continuous LCC periods, inconsistent definitions and terms between land use and land cover, and lastly, the use of different spatial and mathematical models for generating LCC (Klein Goldewijk & Verburg, 2013; Lawrence et al., 2016).

Meanwhile, the identification of LCC characteristics is important and the most challenging task for the quantification of hydrological impacts. Vegetation type, biomass cover, tree stand age, and the matrix of transition can be classified as characteristics of LCC. Moreover, differences in reference ET (ET_o) between deciduous and evergreen forest areas were not significant (Peel et al., 2010). Numerous forest species can own marginal age-related differences in water consumption, and therefore there was no significant transpiration can be observed between old and newborn forest species (Vertessy et al., 2001). Mostly, canopy cover is commonly utilized for characterizing LCC (Song et al., 2018; Sterling & Ducharne, 2008) and for the impact assessment of LCC on water consumption (Jaramillo et al., 2018; Zhou et al., 2015). In the recent years, hydrological observations showed that agriculture and leaf area change are the key characteristics considering the impact of LCC on actual ET rates in (semi-)arid region.

1.1. Role of leaf area index and barren soil in increased reference evapotranspiration

The leaf area index (hereinafter, LAI) is considered as the dominant indicator in environmental and agricultural research. LAI is vastly utilized to monitor the crop growth, and to optimally manage and forecast the yield in agricultural crop production (Gundalia & Dholakia, 2017). LAI is also used as a crucial systemic characteristic intimately relevant to the crop population size and crop yield (Alexandris & Proutsos, 2020). Aligning with that several explorations have contributed to the clarification of the relationship between LAI and crop yield, canopy density and structure (Jabloun & Sahli, 2008; Wang et al., 2019). These investigations revealed that LAI increases with reference to increasing of crop density. Here, the optimum crop density is used to optimize canopy structure (Vanderlinden et al., 2004). Yet, increased biomass density can cause a high LAI, leading to self-shading and yield loss due to the competition for soil nutrients, solar radiation, water, and mineral and organic fertilizers (Almorox et al., 2015; Awal et al., 2020). Furthermore, previous surveys have reported that the ET_o rate between different biomass densities can supervened the LAI differences (Kwon & Choi, 2011; Samani, 2000). Agricultural crop yield and ET_o assist to determine the efficiency of water use. Thus, the determination of optimal LAI can be subject to water use efficiency and crop yield.

1.2. Climate driven factors for increased reference evapotranspiration

According to climatic conditions, in (semi-)arid regions of the planet, agriculture endures the quantity and quality issues of water resources (Li et al., 2018). Agricultural water demand straightforwardly relies on crop pattern and ET_o, hence it is salient to settle the correct value of ET_o for agricultural surveys such as managing and designing irrigation systems, sustainable management of water resources, and simulating crop production (Talebmorad et al., 2021).

Under global climatic variations, the tendency for the ET_o rate and its link with climatic factors are extensively pondered (Croitoru et al., 2020; Irmak et al., 2012; Nagler et al., 2021; Roderick & Farquhar, 2004). Engrossingly, Ghassemi et al. (1995) discovered that whilst surface temperature repeatedly increased, evaporation from land surface at the same time decreased. In the past decades, numerous scientists have briefly investigated the side effects of climatic variations on the spatio-temporal features of ET_o (Nagler et al., 2020; Speranskaya, 2016; Xu et al., 2006). For instance, ET_o has gradually decreased in the majority (semi-)arid countries, and it was assumed that this decrease could be caused by reduced solar radiation and wind speed (Nouri et al., 2020; Zhang et al., 2016; Zhao et al., 2016). An increase in the ET rate was due to the reduced relative humidity and increases in wind speed in some regions (Abbasi et al., 2021; Burn & Hesch, 2007; Dinpashoh et al., 2011; Jarchow et al., 2022).

Additionally, scientists concluded that ET_o is severely influenced by land use change indicators such as LAI (Sun et al., 2008). This was believed and as evidenced above that LCC had higher impact on global water cycle than climatic variations (Xu et al., 2006) and this may mask the climate change effects (Hao et al., 2015).

The vulnerability of diverse ET_o models to the signals of global climate change was evaluated in a semi-arid region (Sabziparvar, 2009). Potential findings of this investigation

demonstrated that the majority of ET_o models manifested the most severe sensitivity to solar radiation (in the short-term) and surface temperature (in the long-term). Considering 10% potential change in climate factors throughout the growing season of agricultural crops, scholars anticipated that an increase in surface temperature can cause a ~8% growth in ET_o in 2050 (Singh et al., 2016). Moreover, the susceptibility of ET to surface temperature and atmospheric rainfall was explored within the historical period from 1970 to 2006 (Chaouche et al., 2010). Mann-Kendall approach (non-parametric) was applied to examine the potential significance of trend in climate factors in this study. The Hargreaves-Samani method was utilized to calculate the ET_o from agricultural land. Eventually, results revealed an upward trend in yearly records of surface temperature and ET.

1.3. Relevant global and local studies

Numerous ET estimation methods and models exist to scrutinize the possible factors that contribute to ET_o (Shao et al., 2019; Zhou et al., 2019) and hydrological modelling (Yang et al., 2021). These two approaches are compounded and still demand a substantial knowledge of soil properties such as soil texture, resistance, soil moisture, and particle diameter and ecological and physiological indicators of canopy such as roughness and stomatal conductance (Dey & Mishra, 2017). Listed indicators are usually hard to derive in data-scarce regions. Since these approaches are considered as process-based and their results mainly depend on generated hypotheses, often, their outputs ranges notably from each other (Zhang et al., 2016; Zhao et al., 2015). Moreover, scientifically inadequate long-term observations hinders the calibration and validation of model-based estimations and restricts the complete understanding of mechanisms at play (Li et al., 2018). Still, the Hargreaves-Samani (hereinafter, HS) framework renders a widely applicable method to split the contributions of sole indicators to global hydrological cycle (Jiang et al., 2015; Yang et al., 2021).

Correspondingly, the HS has experienced large-scale application in partitioning the contributions of hydrological indicators. For instance, the HS framework was applied for quantifying the streamflow response to soil degradation in China (Yang et al., 2020). Teuling et al. (2019) utilized this approach for determining the possible climate change impacts, afforestation, and urbanization on ET_o in Europe. Besides that, an analysis-based solution for the impact of LCC on hydrological subdivision was proposed upon the HS approach (Ning et al., 2020). The output of these investigations has rendered a universal system to tackle with the climate and land surface change impacts on hydrological processes. As having the previous insufficient long-term ET_o observations or valid ET_o sources, few scientific contributions have addressed to dividing the ecological and environmental change impacts on ET_o.

In the case of Uzbekistan, this country is perceived as the biggest irrigation farming country in Central Asia. The proper determination of crop water demand can intervene the massive wastage of surface water which is common in Uzbekistan (Duchemin et al., 2006; Stancalie et al., 2010). To minimize or economize the water use in Uzbekistan (Khaydar et al., 2021), systematical irrigation of the crops is essential based on their physical water demand, including potential ET (Abdullaev et al., 2009; Conrad et al., 2020). Nationwide, the FAO CROPWAT model is a frequent approach to calculate the real crop water consumption considering its practicability (Allen et al., 2005; Srivastava et al., 2020; Tan & Zheng, 2019).

At a national level, ET_o and crop water demand in Uzbekistan throughout 2004–2017 were evaluated using the FAO Penman–Monteith method and the net irrigation requirement was also reported (Khaydar et al., 2021). Moreover, the modified ET_o HS equation was also applied to estimate ET_o in a typical arid zone in the southern Uzbekistan (Gafurov et al., 2018). In this investigation, there was a lack of data on humidity, solar radiation, and wind speed due to outdated technical capacity in line with financial restrictions of local weather stations. Therefore, this research has not been fully finalized that created an opportunity to conduct this actual research. Calculating ET_o has nowadays a greater importance for wholly comprehension of water cycle in Uzbekistan (Gafurov et al., 2018). As far as ET-based irrigation systems are commonly embraced by local water consumers' associations, this can enable increased water savings that could be rerouted to further expand agricultural lands under the risk of global famine possibly emanated from the current geopolitical conflicts and rehabilitate national ecosystem.

Considering all the above, the aim of this paper is to gain further knowledge of the drivers of the high and actual ET_o rate by addressing the following objectives: (1) creating initial and perennial LULC maps; (2) first time mapping LAI in the agricultural land; (3) mapping the perennial solar radiation data; and finally, (4) measuring perennial ET_o of a typical arid region of Uzbekistan using the HS approach.

2. Study area

Uzbekistan, a land-locked country (Fig. 1), is located in the heart of Central Asia sandwiched between the Amu Darya and the Syr Darya rivers. The country's entire land area is 447,400 km^2, with roughly 43,000 km^2 utilized for agricultural purposes. The geography of Uzbekistan is characterized by large lowlands and deserts, as well as foothills and mountain ranges. Because of its geolocation, Uzbekistan experiences dry and continental weather throughout the year, and thus classifying as a (semi-)arid region (Khasanov et al., 2022). Uzbekistan has a distinct climate, with long and dry summers, cool and moist falls, and severe winters (Ivushkin et al., 2017). In the peak summer time (July), the average air temperature reaches 28°C, while it drops 1°C in January. The average sum of yearly atmospheric precipitation is around 430 mm (Ivushkin et al., 2017).

Karakalpakstan (officially known as The Autonomous Republic of Karakalpakstan) is located in northwest Uzbekistan, specifically southeast to southwest of the Aral Sea (Fig. 1). Karakalpakstan is esteemed the lodestone of the Aral Sea Catastrophe where socio-economical and ecological problems are arisen and certainly acute

Fig. 1. Location of study area

(Begdullayeva et al., 2007). Moreover, Karakalpakstan shares its borders with the Kyzylkum Desert to the northwest, the Amu Darya River delta and the Ustyurt Plateau to the southeast. Deserts and semi-deserts define its landscape and comprise around 40% of the entire region. Karakalpakstan is the biggest administrative region according to its territory in Uzbekistan, covering the area of 165,000 km^2. Karakalpakstan is home to roughly 1.8 million (5.9% of the total population of Uzbekistan), whereas approximately a half of the residents inhabit in rural areas. As its climate is semi-arid and sharply continental, hot and dry summer and drizzling winter weathers can be observed. The average annual air temperature is +9°C, followed by the average minimum of −12°C (absolute minimum recorded −40°C) and the average maximum of +35°C (absolute maximum recorded +46°C) (Begdullayeva et al., 2007). Perennial mean of the total atmospheric precipitation is 160 mm, majority falling in winters and early spring. The regional agricultural activities is only possible with irrigation. Karakalpakstan has about 500,000 hectares (ha) of arable land (~3% of its total territory) that is prone to agricultural threats such as soil salinization, unsustainable agricultural activities, rising highly-mineralized groundwater, irrigation mismanagement and unfunctional drainages, and seasonal and long-term drought and sandstorm (Begdullayeva et al., 2007).

3. Data acquisition

3.1. Remote sensing data

Spatial data analyzed in this research were derived by MODIS from Google Earth Engine (hereinafter, GEE). GEE allots remotely sensed imagery available for global public that can be operated a diversity of (non-)educational purposes. For long-term LCC analysis, the MODIS Terra imagery was utilized. This imagery was the 16-day 250 m spatial resolution image for land cover analysis (MCD13Q1) (Ituen & Hu, 2021) and the 500 m spatial resolution for solar radiance (MOD09A1.006) (Li et al., 2021). Simple interpolation method (Inverse Distance Weighting) was undertaken for void filling on both spatially and temporally. The MODIS dataset with a total of 42 satellite images (21 images for the period 2001-2021 in April, when winter wheat reaches its maximum biomass; 21 images for the period 2001-2021 in August, when cotton reaches its maximum biomass) was utilized for LCC and LAI maps. The derived data in GEE have as usual undergone preprocessing stages. LCC and LAI mapping was conducted with the GEE code editor (GISGeography, 2022), Erdas Imagine 2020 (Hexagon, 2020), and ArcMap 10.8 (Redlands, 2020). Notably, though Normalized Difference Vegetation Index (hereinafter, NDVI) and Soil-Adjusted Vegetation Index (hereinafter, SAVI) were employed considering their historical success as affirmative measurement tools on vegetation monitoring, our approach could support other findings, such as LAI and solar radiation, which were explored in latter sections below.

Preliminary image pre-processing was performed to remove the unfavorable voids, systematically created by atmospheric obstrusions. The MODIS Terra imagery at 250 m spatial resolution was readjusted considering atmospheric conditions (e.g., aerosols, gasses, and Rayleigh scattering) (Ituen & Hu, 2021). Similarly, The MODIS Terra imagery at 500 m spatial resolution from GEE comprises

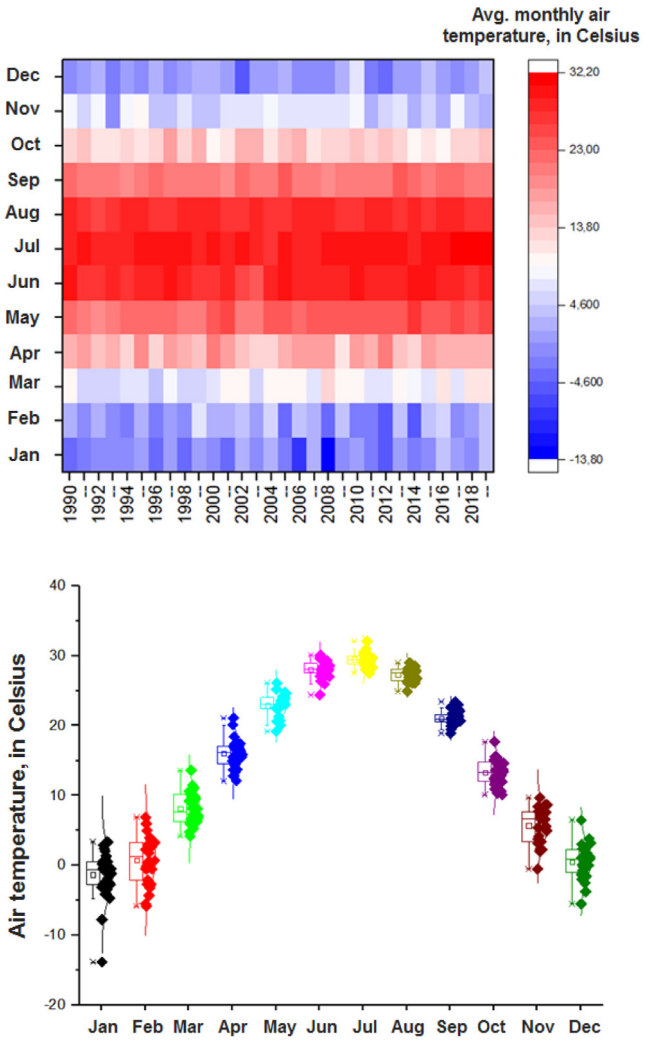

Fig. 2. Air temperature records of Karakalpakstan

atmospherically readjusted bi-directional reflectance, having been masked for clouds, heavy aerosols, water, and cloud shadows. The next step of image pre-processing was to smooth input data by removing potential atmospheric noises. In our paper, we applied a Savitzky-Golay filter (Ituen & Hu, 2021), asymmetric Gaussian, and (double) logistic smoothing as a smoothing tool.

3.2. Climate factors

In regards to the long-term weather observation dataset from 2001 to 2021 (Uzhydromet (Center of Hydrometeorological Service of the Republic of Uzbekistan), 2021) registered in the weather towers in Karakalpakstan, the perennial average air temperature of July or the peak summer time exceeds +30°C, whereas in January (the peak winter time) it is nearly -2°C (Fig. 2). Mean annual sum of long-term atmospheric precipitation was around 160 mm. Considering these climatic conditions and vast majority part of agricultural lands is irrigated in Karakalpakstan, the growing season usually starts from April and ends in October.

4. Data analysis

4.1. Land cover change analysis and solar radiation

As discussed above, the LCC detection in our research was conducted over 21 years, beginning in 2001, using MODIS data to evaluate the severity of changing dynamics in land cover every year. Yet, we plotted maps in this paper for every five years. A tool of super pixels as the reference for analysis to detect and track LCC was employed in lieu of the conventional pixel-based approaches (Jenicka, 2021). Additionally, we used Java scripting to plot the final LCC maps. On the other hand, an arbitrary neighborhood surrounding each pixel in the remotely sensed image was used as samples, for which pixel value could not come after the random distribution. To measure the true size of super pixels, a semivariogram was utilized to

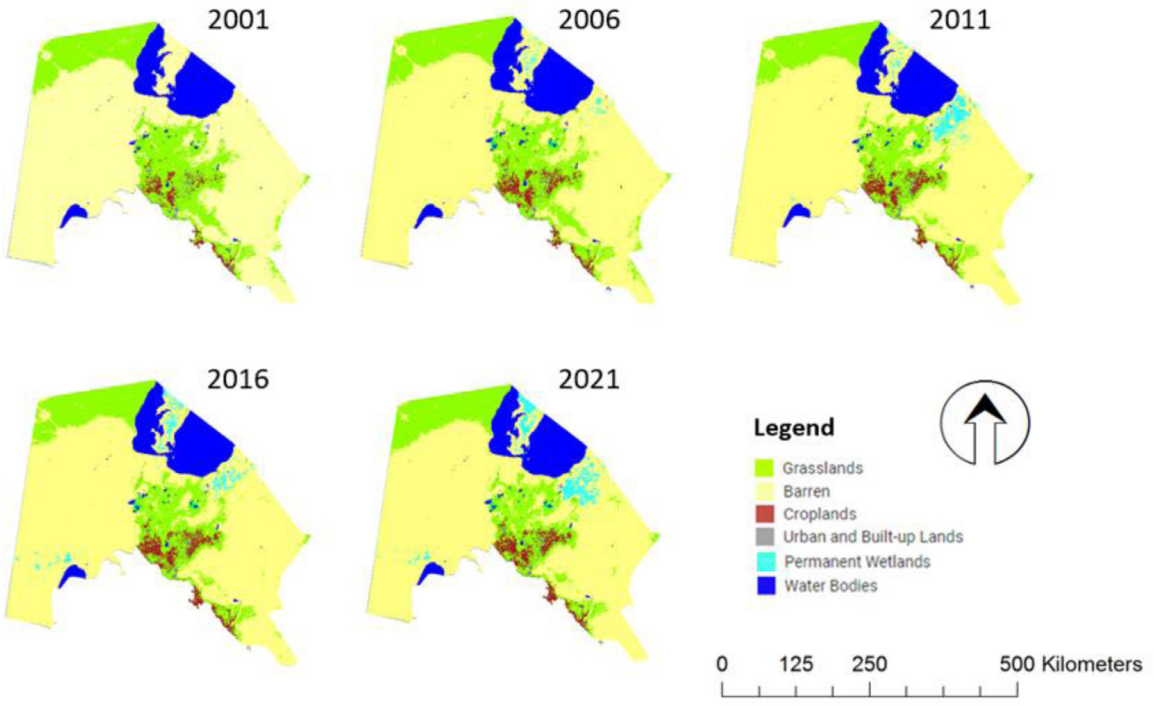

Fig. 3. Land use and land cover change maps of Karakalpakstan (Uzbekistan) through 2001-2021

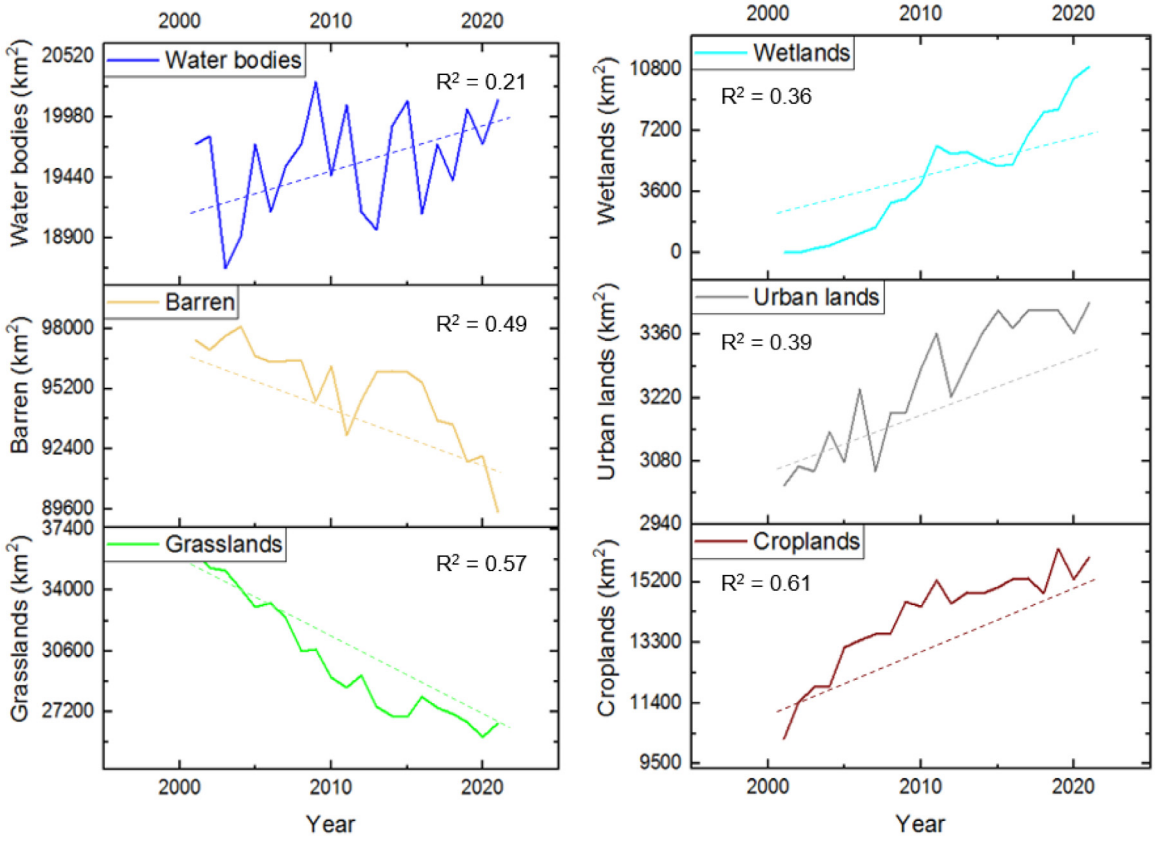

Fig. 4. Changing direction of land use and land cover classes in Karakalpakstan throughout 2001-2021

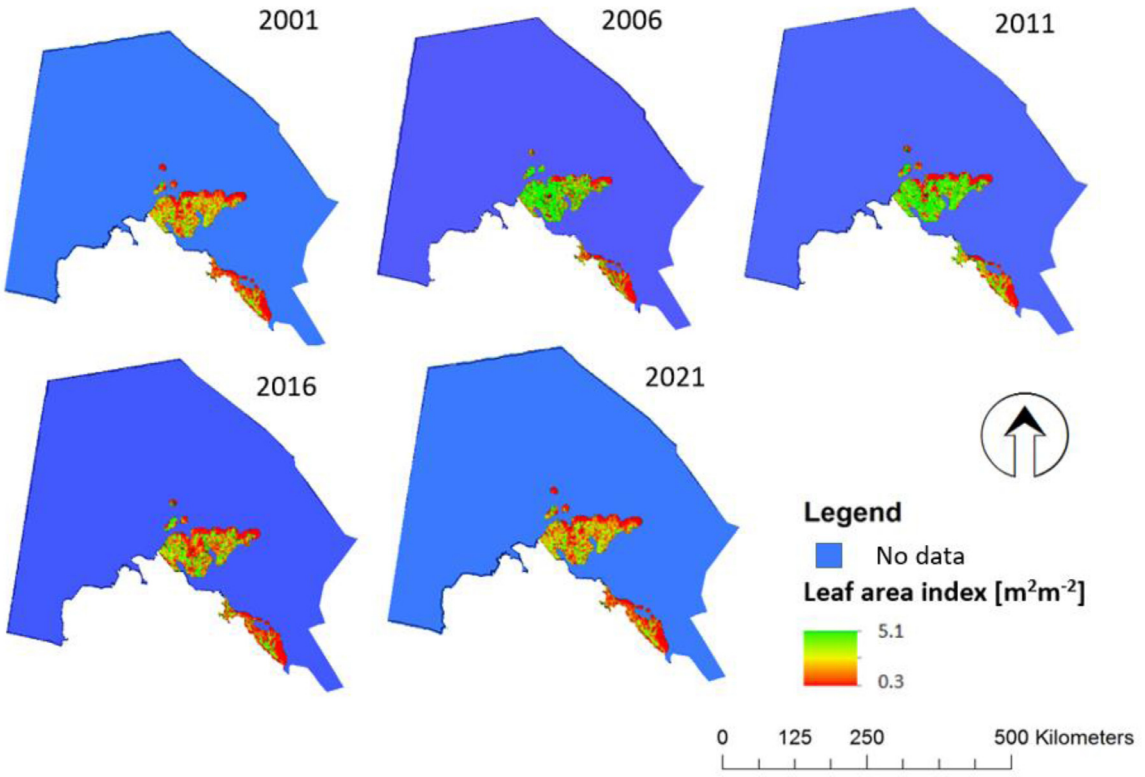

Fig. 5. Leaf area index maps of the agricultural land of Karakalpakstan (Uzbekistan) from 2001 to 2021

analyze the spatial variations of Karakalpakstan displayed in the MODIS data. As the input to used semivariogram, the first principal component of the MODIS dataset was served. Hinged on the first three principal components of MODIS dataset that cover the entire optical bands, the super pixels were derived.

In regards to solar irradiance, we used an existing framework to evaluate and measure daily average net solar radiation clear and cloudy sky conditions through using the MODIS data, onboard from the Terra satellites. The most reliable, Bisht et al. (2005) approach is employed for the portion of clear sky of the MODIS overpass, on the other hand for cloudy sky portion of the MODIS overpass an extension of Bisht et al. (2005) framework was utilized. This extension of Bisht et al. (2005) framework uses the MODIS cloud data imagery (i.e., MOD06_L2) for cloud fraction, cloud top temperature, cloud optical thickness, cloud emissivity, and surface temperature for cloudy days. Through this methodology, we build first solar irradiance map for Karakalpakstan in this paper.

4.2. Leaf area index

After having obtained the multispectral images using MODIS from GEE, the agricultural land of Karakalpakstan was extracted by using vegetation indices (i.e., NDVI). We then converted the output of vegetation indices to LAI for each year (Ma et al., 2021). By using Java script in the GEE code editor, we calculated LAI for Karakalpakstan according to Equation (1).

$$LAI = Total\ leaf\ area \cdot Land\ area^{-1} \quad (1)$$

4.3. Vegetation indices

Two vegetation indices, including NDVI and SAVI were studied. As evidenced, the NDVI is the most commonly and globally used vegetation index Shammi & Meng, 2021). It is defined as (2):

$$NDVI = (NIR - -RED) \cdot (NIR + RED)^{-1} \quad (2)$$

where, *RED* and *NIR* – atmospherically adjusted reflectance in the red and near infrared bands.

To compare with NDVI, SAVI has a soil-adjusted factor diverted to alleviate noises caused by several soil scattering (Bannari et al., 1995). Here, this soil-adjusted factor is alluded to as "L". SAVI is defined by the following Equation (3):

$$SAVI = (NIR - RED) \cdot (1 + L) \cdot (NIR + RED + L)^{-1} \quad (3)$$

where, *L* – soil-adjusted factor of SAVI. An optimal value, which is equal to 0.5, is recommended by Huete (1988).

Once we located green vegetation and calculated LAI for the agricultural land of Karakalpakstan, our next step was to identify the barren soil areas. This was performed by extracting the agricultural land by masking the vegetation cover. The open areas were then classified as a barren soil.

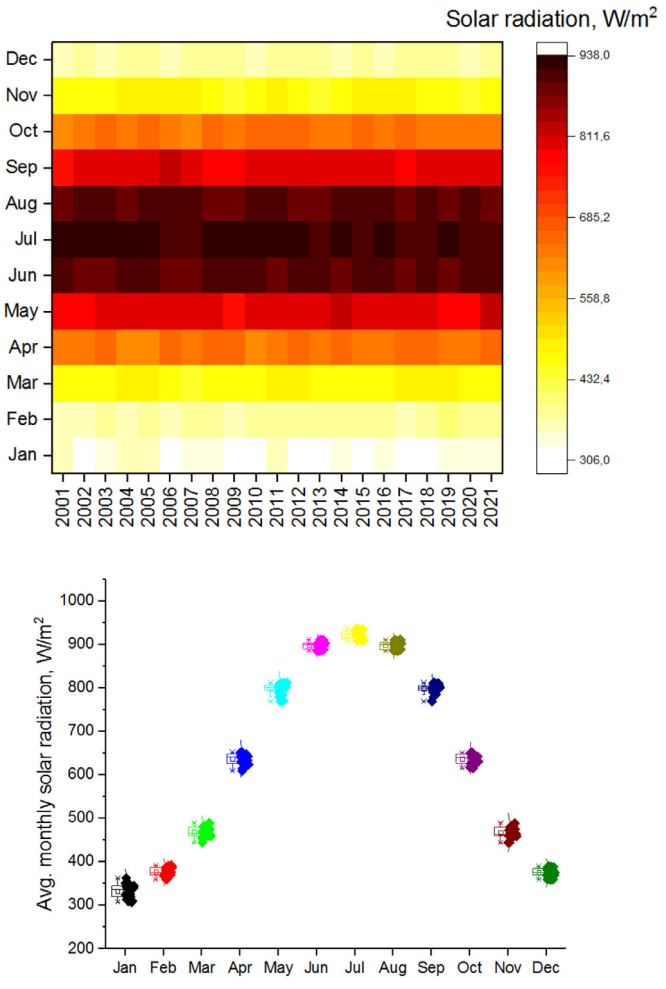

Fig. 6. Solar radiation map of Karakalpakstan (Uzbekistan) within 2001-2021

4.4. Hargreaves-Samani method

The HS equation (Talebmorad et al., 2020) demands decreased observations, with only solar irradiance, maximum air temperature and minimum air temperature for calculation of ET_o (Equation 4):

$$ET_oHS = 0.0135 \cdot k_{Rs} \cdot R_a \sqrt{T_{max} - T_{min}} \cdot (T_a + 17.8) \quad (4)$$

where, 0.0135 – conversion factor from American to the International system of units; k_{Rs} – coefficient of radiation adjustment (commonly, $k_{Rs} = 0.17$ is applied); R_a – daily solar irradiance; T_{max} – maximum air temperature; T_{min} – minimum air temperature; and, T_a – average daily air temperature.

4.5. Evaluation

To evaluate the HS results, the relative error percentage (hereinafter, REP), the root mean square error (hereinafter, RMSE), and coefficients of determination were employed in this paper. The equation for RMSE is given below (Equation 5):

$$RMSE = \sqrt{\frac{\sum_{i=1}^{n} (P_i - O_i)\hat{}2}{n}} \quad (5)$$

where, P_i – predicted values of ET_0HS; O_i – observed ET values; and, n – total number of records.

5. Results and discussion

5.1. Creation of land use and land cover map for Karakalpakstan

Human-induced factors and activities can have a potential to adversely influence the global water cycle, thus affecting ET_o in a region of Karakalpakstan. LCC directly and, somewhat, indirectly reflects how damaging the anthropogenic activity in an area is. The footprint of LCC on ET_o in a particular region mostly originates from physical changes to the surface, affecting the ET_o efficiency (Dias et al., 2015; Douglas et al., 2009). In this section, the reclassified MODIS LULC map of Karakalpakstan (Fig. 3) throughout 2001-2021 demonstrates that: (1) grasslands

are mainly located in the northwestern and central part of the region; (2) barren lands are as the predominant feature class in the maps located in the western and eastern part of the study area; (3) croplands in the study area are remarkably dynamic over time: in 2001 these lands occupied minority territory of the region, but after having massive implementation of policy-induced agricultural practices in Uzbekistan (i.e., land owning), these areas have expanded from 10,300 km^2 to 17,150 km^2 between 2001-2021; (4) areas under urbanization over 21 years in the region were almost invisible in the maps (~3,400 km^2); (5) initially, wetlands did not exist in 2001, however, after 2006, wetlands have significantly expanded over time by 10,600 km^2. This was assumed to become one of the serious consequences of the Aral Sea Catastrophe; and, (6) engrossingly, areas under water were almost stable over time. Since the huge bulk (eastern part) of the Aral Sea has been dried up, the codes created by Java script revealed a water body in this territory. This can be occurred due to two reasons: (1) misclassification/insufficient ground truth data and (2) coding is extremely sensitive to swamp by systematically converting this area into water.

Fig. 4 exhibits the changing direction in the proportions of LULC types in Karakalpakstan within 2001–2021 ($p < 0.01$). Water bodies in the LCC maps covered approximately 19,700 km^2 area in 2001, after having experienced oscillations, in 2021 this figure was 20,500 km^2. The same tendency was also observed in the relevant study conducted by Aslanov et al. (2021). Here, we propose to conduct the sensitivity analysis of coding in Java script to detect LCC as a separate study. Since our main interest by this research expresses on the agricultural land of the region, we did not fully investigate the coding sensitivity. Regarding the barren land, in 2001 this class of LULC occupied almost 97,400 km^2, by experiencing a dramatic downward tendency, by 2021 this class outnumbered as around 89,500 km^2. The significance of barren land in this study is to track whether due to which land cover feature it increased or decreased. This can be perceived that the dramatic shrinkage of barren land in the region was massively due to the conversion to grassland surrounding the former Aral Sea shoreline (Novitskiy et al., 2021). Grasslands, on the other hand, as barren land declined remarkably. This territory was around 36,100 km^2 in 2001, and decreased by 27,400 km^2 in 2021. As grasslands expanding in the barren lands, from other side, these lands have been owning for agricultural purposes, by converting these lands to croplands in the region. In regards to wetlands, until 2006, this class did not exist or could hardly be differentiated in the LULC maps. However, in 2011 wetlands sharply expanded, and this expansion has continued by 2021, occupying almost 10,500 km^2. As urban lands were almost invisible in the maps, if we refer to Fig. 4, we can see there has been a gradual increase in the urbanized territory, taking place on extra 400 km^2 within 21 years. Lastly, croplands were in roughly 10,000 km^2 in 2001, this figure rose by around 16,000 km^2 by 2021.

The LCC maps created above could serve as an imput to calculate the LAI values from agricultural/crop lands of the study area. This could contribute to locating the croplands according to the type of agricultural crops, and eventually, calculating the crop evapotranspiration considering the chosen types of crops in the future studies.

5.2. Measuring Leaf Area Index for Karakalpakstan

Since in Karakalpakstan the main crop types are cotton and winter wheat, the LAI calculations were performed separately for cotton (August) and winter wheat (April) using NDVI first, and then, SAVI to further enhance the results by removing soil noise. The output LAI maps were then stacked together to generate one single map. The LAI change in the agricultural land of Karakalpakstan showed a sharp decrease (2001) – gradual increase (2011) – steep decrease (2021) over 21 years (Fig. 5). From the figure, the northern part of the study area experienced restricted LAI 0.5 m^2m^{-2} in 2001, despite having a slight increase (LAI 1.1-3.5 m^2m^{-2}), by 2021 the tendency showed the same result (LAI 0.5 m^2m^{-2}) as recorded in 2001. In the central part of the agricultural land of the region the LAI values were pretty dynamic ranging from LAI 2.5 m^2m^{-2} to its maximum LAI 5.1 m^2m^{-2} throughout 21 years. By this tendency, we can assume that this part of the agricultural land is the most suitable for agricultural practices according to Stewart & Peterson (2015). In the southern part of the agricultural land of the region the LAI values relatively low, varying from LAI 0.3 m^2m^{-2} to LAI 1.2 m^2m^{-2}. Interestingly, some parts of this area of interest had increased LAI values (4.0-4.7 m^2m^{-2}), still becoming unsuitable land for agriculture (Stewart & Peterson, 2015).

5.3. Measuring perennial solar radiation

As Karakalpakstan is located in a typical dryland of the world, due to its geographical location, the sun shine is extremely abundant. The average sunny days in Karakalpakstan are 260 days in a year (Kulmatov et al., 2018). Therefore, in some circumstances, we can witness that agricultural crops have stopped developing because of excessive solar irradiance. To measure radiation, we used Bisht et al. (2005) methodology to mask the solar irradiance from MODIS dataset. This was conducted firstly in the case of Karakalpakstan. As this indicator takes an important role in the ET calculation, we plotted average monthly solar irradiance reaching the agricultural land of Karakalpakstan (Fig. 6).

As visualized above, the agricultural land in the region receives excessive solar radiation in July (> 900 W/m^2). The sparsest solar irradiance can be observed in January with an average of 330 W/m^2. The distribution of solar radiation across the agricultural land of the study area was decently certain over time. To assume, there is no side effect of climatic variation on solar radiation. However, increased solar irradiance over-burns crops, leading to a decrease in crop yield (Cossu et al., 2014).

5.4. Measuring ET_o for croplands of Karakalpakstan

ET_o intensity is mutually influenced by solar radiation, air temperature, and crop LAI (Yang et al., 2022). Fig. 7 illustrates calculated average monthly ET_o values using the ET_oHS approach from 2001 to 2021. As an input,

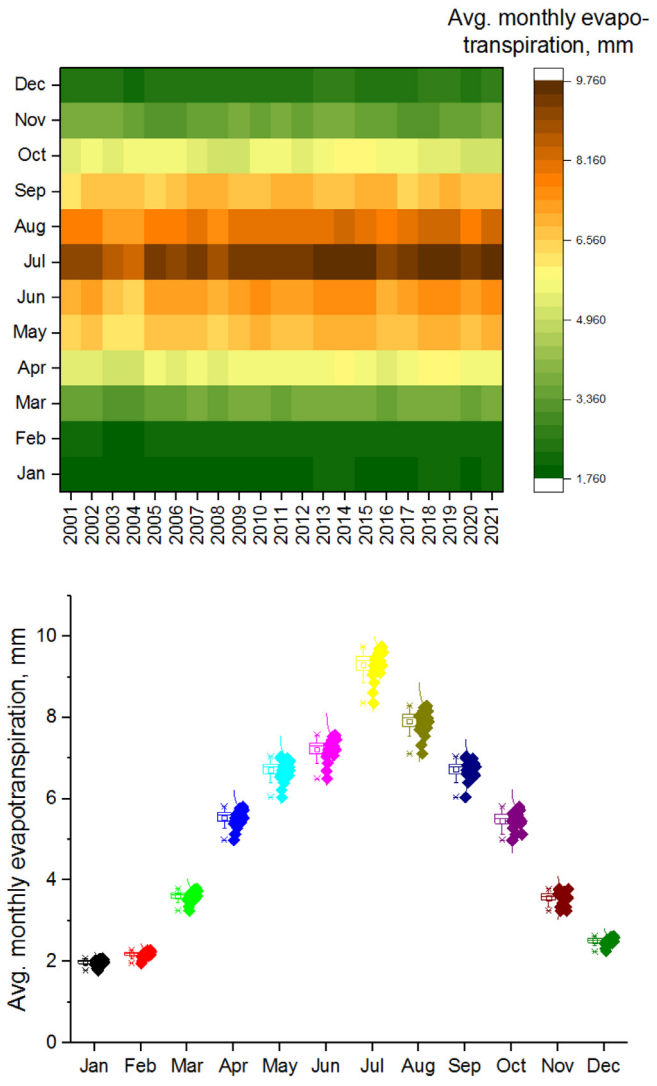

Fig. 7. ET_o from the agricultural land of Karakalpakstan (Uzbekistan) within 2001-2021

all the elements to fulfill the HS equation were formed in the average monthly values. For the maximum and minimum air temperatures, we considered the average perennial minimum and maximum values recorded in the weather stations in the study area.

In regards to our findings, the tendency for ET_o was not dynamic so far over time as observed in solar radiation maps above. Besides, we executed a simple correlation analysis between LAI and calculated ET_o and we found that these two variables are slightly correlated each other ($R = 0.57$). This contradicts the research results by Lima et al. (2013), who identified overestimates of ET_o values in the HS approach in contrast to other ET calculation methods in Brazil. As air temperature (Fig. 2), the average monthly maximum ET_o rate in agricultural lands was observed in July with almost 10 mm, while the average monthly minimum was recorded in January with around 2 mm. Moreover, the mean approximate relative error percentage of ET_oHS throughout the experimental years outnumbered 12%, 15%, 14% and 10% in four seasons, respectively. In the similar investigations conducted in Uzbekistan, the annual ET_o for the year of 2016 accounted for 1,573 mm with 8.87 mm/day (maximum) and 1.25 mm/day (minimum) (Gafurov et al., 2018). Another similar research was conducted in the neighboring Khorezm province of Uzbekistan by Awan et al. (2011), in which the HS method revealed 1,375 mm ET_o with 7.36 mm/day (maximum) in July and 0.64 mm/day (minimum) in January for long-term analyses from 1987 to 2005.

Regarding the ET_o estimations, the correlation between average monthly ET_oHS and LAI values of crops was sufficiently high with R^2 of 0.77 in 2001, 0.82 in 2011, and 0.79 in 2021, and as an indicator showing the statistical significance, *p*-values were far below 0.01. With respect to the decreased values of RMSE (~0.09), the ET_oHS method that was failed to put into practice in Kashkadarya province of Uzbekistan (Gafurov et al., 2018) can now be utilized to estimate the potential ET_o from agricultural land. Specifically,

the RMSE of ET_oHS were ~0.06 in 2001, ~0.07 in 2011, and ~0.14 in 2021.

6. Conclusions

By the multifactorial analyses of the perennial air temperature, LCC, LAI, solar irradiance, and ET in a typical dryland of Uzbekistan, we found that increased crop density in agriculture and the conversion of barren soil to grasslands to rehabilitate the seashore ecosystem of the Aral Sea significantly influenced LAI. Tracking the perennial spatial changes in the LAI area in Uzbekistan has not previously been investigated. Therefore, this research could contribute to the general understanding of the LAI environment of Uzbekistan and we designed a simpler approach to calculate LAI hinged on the values of the vegetation indices. It is evident to note that there is no role of LAI in the ET_0 estimation, but with this study we stepped forward to formulate the input variable (LAI) to calculate crop evapotranspiration which will be investigated in our future research. Yet, we witnessed that the LAI expansion in the agricultural land of Karakalpakstan slowly accelerated the ET_o rate ($R = \sim 0.6$) that was the key influencer of an increase in crop water demand. Interestingly, we can witness that measured solar radiation and ET_o were certain over time, by showing the almost identical values for each..

According to our findings, the ET_oHS method is highly applicable for estimating regional ET_o in the agricultural land under arid continental climate. The main advantage of the HS method for successfully running the ETo estimation in this study was the straightforward equation, without requiring model outputs. Measuring ET_o is crucial for ultimately intervening and getting deeper insight into the water balance of natural systems, especially for large-scale irrigated areas. This is necessary in regional water management, as water resources must be clearly handled from the river basin through irrigated fields. If irrigation considering ET is extensively adopted by Uzbek water consumers, it can reflect on greater water savings that can be transferred to develop and rehabilitate agricultural and ecological status of the region. Furthermore, the findings show that the HS method used in our investigation can be utilized to measure potential ET_o in data-scarce regions and to anticipate future ET_o values based on global climate models according to observed low RMSE values. This will assist to inform and facilitate decision-making in agriculture and implement more effective agricultural practices in irrigation scheduling, water management, and crop production.

Declaration of Competing Interest

The authors declare that they have no known competing financial interests or personal relationships that could have appeared to influence the work reported in this paper.

CRediT authorship contribution statement

Umida Makhmudova: Conceptualization, Resources, Methodology, Investigation, Writing – original draft. **Sayidjakhon Khasanov:** Software, Formal analysis, Data curation, Writing – review & editing. **Akmal Karimov:** Supervision, Writing – review & editing. **Sarvar Abdurakhmonov:** Visualization, Writing – review & editing.

Ethical approval

The present research does not involve studies with human participants and/or animals performed by any of the author.

Acknowledgment

This research was performed as a partial fulfilment of PhD studies at “Tashkent Institute of Irrigation and Agricultural Mechanization Engineers” National Research University, Uzbekistan

Funding

Not applicable

Data availability

Not applicable

Consent to participate

All the authors agree to submit the manuscript to the renowned journal “Ecohydrology and Hydrobiology”

Consent for publication

The manuscript is original. It has not been published previously by any of the author and even not under the consideration in any other journal at the time of submission.

References

Abbasi, N., Nouri, H., Didan, K., Barreto-Muñoz, A., Chavoshi Borujeni, S., Salemi, H., Opp, C., Siebert, S., Nagler, P., 2021. Estimating Actual Evapotranspiration over Croplands Using Vegetation Index Methods and Dynamic Harvested Area. Remote Sensing 13 (24), 5167. doi:10.3390/rs13245167.

Abdullaev, I., De Fraiture, C., Giordano, M., Yakubov, M., Rasulov, A., 2009. Agricultural Water Use and Trade in Uzbekistan: Situation and Potential Impacts of Market Liberalization. International Journal of Water Resources Development 25 (1), 47–63. doi:10.1080/07900620802517533.

Adane, Z.A., Nasta, P., Zlotnik, V., Wedin, D., 2018. Impact of grassland conversion to forest on groundwater recharge in the Nebraska Sand Hills. Journal of Hydrology: Regional Studies 15, 171–183. doi:10.1016/j.ejrh.2018.01.001.

Alexandris, S., Proutsos, N., 2020. How significant is the effect of the surface characteristics on the Reference Evapotranspiration estimates? Agricultural Water Management 237, 106181. doi:10.1016/j.agwat.2020.106181.

Allen, R.G., Pereira, L.S., Smith, M., Raes, D., Wright, J.L., 2005. FAO-56 Dual Crop Coefficient Method for Estimating Evaporation from Soil and Application Extensions. Journal of Irrigation and Drainage Engineering 131 (1), 2–13. doi:10.1061/(ASCE)0733-9437(2005)131:1(2).

Almorox, J., Quej, V.H., Martí, P., 2015. Global performance ranking of temperature-based approaches for evapotranspiration estimation considering Köppen climate classes. Journal of Hydrology 528, 514–522. doi:10.1016/j.jhydrol.2015.06.057.

Aslanov, I., Khasanov, S., Khudaybergenov, Y., Groll, M., Opp Ch, C., Li, F., Del-Valle, E.R., 2021. Land cover-adjusted index for the former Aral Sea using Landsat images. E3S Web of Conferences 227, 02005. doi:10.1051/e3sconf/202122702005.

Awal, R., Habibi, H., Fares, A., Deb, S., 2020. Estimating reference crop evapotranspiration under limited climate data in West Texas. Journal of Hydrology: Regional Studies 28, 100677. doi:10.1016/j.ejrh.2020.100677.

Awan, U.K., Tischbein, B., Conrad, C., Martius, C., Hafeez, M., 2011. Remote Sensing and Hydrological Measurements for Irrigation Performance Assessments in a Water User Association in the Lower Amu Darya River Basin. Water Resources Management 25 (10), 2467–2485. doi:10.1007/s11269-011-9821-2.

Bannari, A., Morin, D., Bonn, F., Huete, A.R., 1995. A review of vegetation indices. Remote Sensing Reviews 13 (1–2), 95–120. doi:10.1080/02757259509532298.

Begdullayeva, T., Kienzler, K.M., Kan, E., Ibragimov, N., Lamers, J.P.A., 2007. Response of Sorghum bicolor varieties to soil salinity for feed and food production in Karakalpakstan, Uzbekistan. Irrigation and Drainage Systems 21 (3–4), 237–250. doi:10.1007/s10795-007-9020-8.

Bisht, G., Venturini, V., Islam, S., Jiang, L., 2005. Estimation of the net radiation using MODIS (Moderate Resolution Imaging Spectroradiometer) data for clear sky days. Remote Sensing of Environment 97 (1), 52–67. doi:10.1016/j.rse.2005.03.014.

Burn, D.H., Hesch, N.M., 2007. Trends in evaporation for the Canadian Prairies. Journal of Hydrology 336 (1–2), 61–73. doi:10.1016/j.jhydrol.2006.12.011.

Chaouche, K., Neppel, L., Dieulin, C., Pujol, N., Ladouche, B., Martin, E., Salas, D., Caballero, Y., 2010. Analyses of precipitation, temperature and evapotranspiration in a French Mediterranean region in the context of climate change. Comptes Rendus Geoscience 342 (3), 234–243. doi:10.1016/j.crte.2010.02.001.

Conrad, C., Usman, M., Morper-Busch, L., Schönbrodt-Stitt, S., 2020. Remote sensing-based assessments of land use, soil and vegetation status, crop production and water use in irrigation systems of the Aral Sea Basin. A review. Water Security 11. doi:10.1016/j.wasec.2020.100078.

Cornelissen, T., Diekkrüger, B., Giertz, S., 2013. A comparison of hydrological models for assessing the impact of land use and climate change on discharge in a tropical catchment. Journal of Hydrology 498, 221–236. doi:10.1016/j.jhydrol.2013.06.016.

Cossu, M., Murgia, L., Ledda, L., Deligios, P.A., Sirigu, A., Chessa, F., Pazzona, A., 2014. Solar radiation distribution inside a greenhouse with south-oriented photovoltaic roofs and effects on crop productivity. Applied Energy 133, 89–100. doi:10.1016/j.apenergy.2014.07.070.

Croitoru, A.-E., Man, T.C., Vâtcă, S.D., Kobulniczky, B., Stoian, V., 2020. Refining the Spatial Scale for Maize Crop Agro-Climatological Suitability Conditions in a Region with Complex Topography towards a Smart and Sustainable Agriculture. Case Study: Central Romania (Cluj County). Sustainability 12 (7), 2783. doi:10.3390/su12072783.

Dey, P., Mishra, A., 2017. Separating the impacts of climate change and human activities on streamflow: A review of methodologies and critical assumptions. Journal of Hydrology 548, 278–290. doi:10.1016/j.jhydrol.2017.03.014.

Dias, L.C.P., Macedo, M.N., Costa, M.H., Coe, M.T., Neill, C., 2015. Effects of land cover change on evapotranspiration and streamflow of small catchments in the Upper Xingu River Basin, Central Brazil. Journal of Hydrology: Regional Studies 4, 108–122. doi:10.1016/j.ejrh.2015.05.010.

Dinpashoh, Y., Jhajharia, D., Fakheri-Fard, A., Singh, V.P., Kahya, E., 2011. Trends in reference crop evapotranspiration over Iran. Journal of Hydrology 399 (3–4), 422–433. doi:10.1016/j.jhydrol.2011.01.021.

Douglas, E.M., Jacobs, J.M., Sumner, D.M., Ray, R.L., 2009. A comparison of models for estimating potential evapotranspiration for Florida land cover types. Journal of Hydrology 373 (3–4), 366–376. doi:10.1016/j.jhydrol.2009.04.029.

Duchemin, B., Hadria, R., Erraki, S., Boulet, G., Maisongrande, P., Chehbouni, A., Escadafal, R., Ezzahar, J., Hoedjes, J.C.B., Kharrou, M.H., Khabba, S., Mougenot, B., Olioso, A., Rodriguez, J.-C., Simonneaux, V., 2006. Monitoring wheat phenology and irrigation in Central Morocco: On the use of relationships between evapotranspiration, crops coefficients, leaf area index and remotely-sensed vegetation indices. Agricultural Water Management 79 (1), 1–27. doi:10.1016/j.agwat.2005.02.013.

Gafurov, Z., Eltazarov, S., Akramov, B., Yuldashev, T., Djumaboev, K., Anarbekov, O., 2018. Modifying Hargreaves-Samani Equation for Estimating Reference Evapotranspiration in Dryland Regions of Amudarya River Basin. Agricultural Sciences 09 (10), 1354–1368. doi:10.4236/as.2018.910094.

Ghassemi, F., Jakeman, A., Nix, N., 1995. Salinization of land and water resources: human causes, extent, management and case studies, Canberra, Australia. CAB International.

Gibson, L., Münch, Z., Palmer, A., Mantel, S., 2018. Future land cover change scenarios in South African grasslands – implications of altered biophysical drivers on land management. Heliyon 4 (7), e00693. doi:10.1016/j.heliyon.2018.e00693.

GISGeography, 2022. *Google Earth Engine: A Quick Guide for Beginners.* Guide.

Gordon, L.J., Steffen, W., Jönsson, B.F., Folke, C., Falkenmark, M., Johannessen, Å., 2005. Human modification of global water vapor flows from the land surface. Proceedings of the National Academy of Sciences 102 (21), 7612–7617. doi:10.1073/pnas.0500208102.

Gundalia, M., Dholakia, M., 2017. Modeling daily reference evapotranspiration in middle south Saurashtra region of India for monsoon season using most dominant meteorological variables and the FAO-56 Penman-Monteith method. MAUSAM 68 (1), 1–8. doi:10.54302/mausam.v68i1.401.

Hahmann, A.N., Dickinson, R.E., 1997. RCCM2–BATS Model over Tropical South America: Applications to Tropical Deforestation. Journal of Climate 10 (8), 1944–1964. doi:10.1175/1520-0442(1997)010⟨1944:RBMOTS⟩2.0.CO;2.

Hao, L., Sun, G., Liu, Y., Wan, J., Qin, M., Qian, H., Liu, C., Zheng, J., John, R., Fan, P., Chen, J., 2015. Urbanization dramatically altered the water balances of a paddy field-dominated basin in southern China. Hydrology and Earth System Sciences 19 (7), 3319–3331. doi:10.5194/hess-19-3319-2015.

Hexagon. (2020). *The World's Preferred Remote Sensing Software Package (Erdas Imagine 2020).* Hexagon Geospatial Products. https://www.hexagongeospatial.com/products/power-portfolio/erdas-imagine

Huete, A., 1988. A soil-adjusted vegetation index (SAVI). Remote Sensing of Environment 25 (3), 295–309. doi:10.1016/0034-4257(88)90106-X.

Irmak, S., Kabenge, I., Skaggs, K.E., Mutiibwa, D., 2012. Trend and magnitude of changes in climate variables and reference evapotranspiration over 116-yr period in the Platte River Basin, central Nebraska–USA. Journal of Hydrology 420–421, 228–244. doi:10.1016/j.jhydrol.2011.12.006.

Ituen, I., Hu, B., 2021. An Automatic and Operational Method for Land Cover Change Detection Using Spatiotemporal Analysis of MODIS Data: A Northern Ontario (Canada) Case Study. ISPRS International Journal of Geo-Information 10 (5), 325. doi:10.3390/ijgi10050325.

Ivushkin, K., Bartholomeus, H., Bregt, A.K., Pulatov, A., 2017. Satellite Thermography for Soil Salinity Assessment of Cropped Areas in Uzbekistan. Land Degradation & Development 28 (3), 870–877. doi:10.1002/ldr.2670.

Jabloun, M., Sahli, A., 2008. Evaluation of FAO-56 methodology for estimating reference evapotranspiration using limited climatic data. Agricultural Water Management 95 (6), 707–715. doi:10.1016/j.agwat.2008.01.009.

Jaramillo, F., Cory, N., Arheimer, B., Laudon, H., van der Velde, Y., Hasper, T.B., Teutschbein, C., Uddling, J., 2018. Dominant effect of increasing forest biomass on evapotranspiration: interpretations of movement in Budyko space. Hydrology and Earth System Sciences 22 (1), 567–580. doi:10.5194/hess-22-567-2018.

Jarchow, C.J., Waugh, W.J., Nagler, P.L., 2022. Calibration of an evapotranspiration algorithm in a semiarid sagebrush steppe using a 3-ha lysimeter and Landsat normalized difference vegetation index data. Ecohydrology 15 (3). doi:10.1002/eco.2413.

Jenicka, S., 2021. Overview of Spatial Data Analysis and Other Land Cover Classification Methods. In: Land Cover Classification of Remotely Sensed Images. Springer International Publishing, pp. 155–164. doi:10.1007/978-3-030-66595-1_8.

Jiang, C., Xiong, L., Wang, D., Liu, P., Guo, S., Xu, C.-Y., 2015. Separating the impacts of climate change and human activities on runoff using the Budyko-type equations with time-varying parameters. Journal of Hydrology 522, 326–338. doi:10.1016/j.jhydrol.2014.12.060.

Jin, Z., Liang, W., Yang, Y., Zhang, W., Yan, J., Chen, X., Li, S., Mo, X., 2017. Separating Vegetation Greening and Climate Change Controls on Evapotranspiration trend over the Loess Plateau. Scientific Reports 7 (1), 8191. doi:10.1038/s41598-017-08477-x.

Khasanov, S., Li, F., Kulmatov, R., Zhang, Q., Qiao, Y., Odilov, S., Yu, P., Leng, P., Hirwa, H., Tian, C., Yang, G., Liu, H., Akhmatov, D., 2022. Evaluation of the perennial spatio-temporal changes in the groundwater level and mineralization, and soil salinity in irrigated lands of arid zone: as an example of Syrdarya Province, Uzbekistan. Agricultural Water Management 263, 107444. doi:10.1016/j.agwat.2021.107444.

Khaydar, D., Chen, X., Huang, Y., Ilkhom, M., Liu, T., Friday, O., Farkhod, A., Khusen, G., Gulkaiyr, O., 2021. Investigation of crop evapotranspiration and irrigation water requirement in the lower Amu Darya River Basin, Central Asia. Journal of Arid Land 13 (1), 23–39. doi:10.1007/s40333-021-0054-9.

Klein Goldewijk, K., Verburg, P.H., 2013. Uncertainties in global-scale reconstructions of historical land use: an illustration using the HYDE data set. Landscape Ecology 28 (5), 861–877. doi:10.1007/s10980-013-9877-x.

Kulmatov, R., Groll, M., Rasulov, A., Soliev, I., Romic, M., 2018. Status quo and present challenges of the sustainable use and management of water and land resources in Central Asian irrigation zones - The example of the Navoi region (Uzbekistan). Quaternary International 464, 396–410. doi:10.1016/j.quaint.2017.11.043.

Kwon, H., Choi, M., 2011. Error assessment of climate variables for FAO-56 reference evapotranspiration. Meteorology and Atmospheric Physics 112 (1–2), 81–90. doi:10.1007/s00703-011-0132-1.

Lawrence, D.M., Hurtt, G.C., Arneth, A., Brovkin, V., Calvin, K.V., Jones, A.D., Jones, C.D., Lawrence, P.J., de Noblet-Ducoudré, N., Pongratz, J., Seneviratne, S.I., Shevliakova, E., 2016. The Land Use Model Intercomparison Project (LUMIP) contribution to CMIP6: rationale and experimental design. Geoscientific Model Development 9 (9), 2973–2998. doi:10.5194/gmd-9-2973-2016.

Li, W., Perera, S., Linstead, E., Thomas, R., El-Askary, H., Piechota, T., Struppa, D., 2021. Investigating Decadal Changes of Multiple Hydrological Products and Land-Cover Changes in the Mediterranean Region for 2009–2018. Earth Systems and Environment 5 (2), 285–302. doi:10.1007/s41748-021-00213-w.

Li, X., Zhang, S., Liu, X., Wang, X., Zhou, A., Liu, P., 2018. Important role of MAMs in bifurcation and coherence resonance of calcium oscillations. Chaos, Solitons & Fractals 106, 131–140. doi:10.1016/j.chaos.2017.11.018.

Lima, J.R.de S., Antonino, A.C.D., Souza, E.S.de, Hammecker, C., Montenegro, S.M.G.L., Lira, C.A.B.de O, 2013. Calibration of Hargreaves-Samani Equation for Estimating Reference Evapotranspiration in Sub-Humid Region of Brazil. Journal of Water Resource and Protection 05 (12), 1–5. doi:10.4236/jwarp.2013.512A001.

Ma, Y., Zhang, Q., Yi, X., Ma, L., Zhang, L., Huang, C., Zhang, Z., Lv, X., 2021. Estimation of Cotton Leaf Area Index (LAI) Based on Spectral Transformation and Vegetation Index. Remote Sensing 14 (1), 136. doi:10.3390/rs14010136.

Nagler, P.L., Barreto-Muñoz, A., Chavoshi Borujeni, S., Nouri, H., Jarchow, C.J., Didan, K., 2021. Riparian Area Changes in Greenness and Water Use on the Lower Colorado River in the USA from 2000 to 2020. Remote Sensing 13 (7), 1332. doi:10.3390/rs13071332.

Nagler, P.L., Barreto-Muñoz, A., Chavoshi Borujeni, S., Jarchow, C.J., Gómez-Sapiens, M.M., Nouri, H., Herrmann, S.M., Didan, K., 2020. Ecohydrological responses to surface flow across borders: Two decades of changes in vegetation greenness and water use in the riparian corridor of the Colorado River delta. Hydrological Processes 34 (25), 4851–4883. doi:10.1002/hyp.13911.

Ning, T., Li, Z., Feng, Q., Chen, W., Li, Z., 2020. Effects of forest cover change on catchment evapotranspiration variation in China. Hydrological Processes 34 (10), 2219–2228. doi:10.1002/hyp.13719.

Nouri, H., Nagler, P., Chavoshi Borujeni, S., Barreto Munez, A., Alaghmand, S., Noori, B., Galindo, A., Didan, K., 2020. Effect of spatial resolution of satellite images on estimating the greenness and evapotranspiration of urban green spaces. Hydrological Processes 34 (15), 3183–3199. doi:10.1002/hyp.13790.

Novitskiy, Z., Hamzayev, A., Bakirov, N., Karimkulov, A., 2021. Study on the development of the desert pasture agrophytocenoses using a wide range of forage plants. E3S Web of Conferences 304, 03021. doi:10.1051/e3sconf/202130403021.

Pan, S., Tian, H., Dangal, S.R.S., Yang, Q., Yang, J., Lu, C., Tao, B., Ren, W., Ouyang, Z., 2015. Responses of global terrestrial evapotranspiration to climate change and increasing atmospheric <scp>CO 2 </scp>in the 21st century. Earth's Future 3 (1), 15–35. doi:10.1002/2014EF000263.

Peel, M.C., McMahon, T.A., Finlayson, B.L., 2010. Vegetation impact on mean annual evapotranspiration at a global catchment scale. Water Resources Research 46 (9). doi:10.1029/2009WR008233.

Pielke, R.A., Pitman, A., Niyogi, D., Mahmood, R., McAlpine, C., Hossain, F., Goldewijk, K.K., Nair, U., Betts, R., Fall, S., Reichstein, M., Kabat, P., de Noblet, N., 2011. Land use/land cover changes and climate: modeling analysis and observational evidence. WIREs Climate Change 2 (6), 828–850. doi:10.1002/wcc.144.

Redlands, C.E.S.R.I., 2020. ArcGIS Desktop: Release 10.8. ESRI.

Roderick, M.L., Farquhar, G.D., 2004. Changes in Australian pan evaporation from 1970 to 2002. International Journal of Climatology 24 (9), 1077–1090. doi:10.1002/joc.1061.

Sabziparvar, A.A., 2009. Estimation of clear-sky effective erythema radiation from broadband solar radiation (300-3000 nm) data in an arid climate. International Journal of Climatology 29 (13), 2027–2032. doi:10.1002/joc.1848.

Samani, Z., 2000. Estimating Solar Radiation and Evapotranspiration Using Minimum Climatological Data. Journal of Irrigation and Drainage Engineering 126 (4), 265–267. doi:10.1061/(ASCE)0733-9437(2000)126:4(265).

Shammi, S.A., Meng, Q., 2021. Use time series NDVI and EVI to develop dynamic crop growth metrics for yield modeling. Ecological Indicators 121, 107124. doi:10.1016/j.ecolind.2020.107124.

Shao, R., Zhang, B., Su, T., Long, B., Cheng, L., Xue, Y., Yang, W., 2019. Estimating the Increase in Regional Evaporative Water Consumption as a Result of Vegetation Restoration Over the Loess Plateau, China. Journal of Geophysical Research: Atmospheres 124 (22), 11783–11802. doi:10.1029/2019JD031295.

Sheil, D., 2018. Forests, atmospheric water and an uncertain future: the new biology of the global water cycle. Forest Ecosystems 5 (1), 19. doi:10.1186/s40663-018-0138-y.

Shukla, J., Mintz, Y., 1982. Influence of Land-Surface Evapotranspiration on the Earth's Climate. Science 215 (4539), 1498–1501. doi:10.1126/science.215.4539.1498.

Singh, A., Singh, M.K., Ghoshal, N., 2016. Microbial Biomass Dynamics in a Tropical Agroecosystem: Influence of Herbicide and Soil Amendments. Pedosphere 26 (2), 257–264. doi:10.1016/S1002-0160(15)60040-6.

Song, X.-P., Hansen, M.C., Stehman, S.V., Potapov, P.V., Tyukavina, A., Vermote, E.F., Townshend, J.R., 2018. Global land change from 1982 to 2016. Nature 560 (7720), 639–643. doi:10.1038/s41586-018-0411-9.

Speranskaya, N.A., 2016. Actual Evaporation from Natural Green Land over European Russia: Available Observations and Restored Data. *Izvestiya Rossiiskoi Akademii Nauk*. Seriya Geograficheskaya 2, 49–60. doi:10.15356/0373-2444-2016-2-49-60.

Srivastava, A., Kumari, N., Maza, M., 2020. Hydrological Response to Agricultural Land Use Heterogeneity Using Variable Infiltration Capacity Model. Water Resources Management 34 (12), 3779–3794. doi:10.1007/s11269-020-02630-4.

Stancalie, G., Marica, A., Toulios, L., 2010. Using earth observation data and CROPWAT model to estimate the actual crop evapotranspiration. Physics and Chemistry of the Earth, Parts A/B/C 35 (1–2), 25–30. doi:10.1016/j.pce.2010.03.013.

Sterling, S., Ducharne, A., 2008. Comprehensive data set of global land cover change for land surface model applications. Global Biogeochemical Cycles 22 (3). doi:10.1029/2007GB002959, n/a-n/a.

Stewart, B.A., Peterson, G.A., 2015. Managing Green Water in Dryland Agriculture. Agronomy Journal 107 (4), 1544–1553. doi:10.2134/agronj14.0038.

Sun, G., McNulty, S.G., Moore Myers, J.A., Cohen, E.C, 2008. Impacts of Multiple Stresses on Water Demand and Supply Across the Southeastern United States 1. JAWRA Journal of the American Water Resources Association 44 (6), 1441–1457. doi:10.1111/j.1752-1688.2008.00250.x.

Talebmorad, H., Ahmadnejad, A., Eslamian, S., Askari, K.O.A., Singh, V.P., 2020. Evaluation of uncertainty in evapotranspiration values by FAO56-Penman-Monteith and Hargreaves-Samani methods. International Journal of Hydrology Science and Technology 10 (2), 135. doi:10.1504/IJHST.2020.106481.

Talebmorad, H., Koupai, J.A., Eslamian, S., Mousavi, S.F., Akhavan, S., Askari, K.O.A., Singh, V.P., 2021. Evaluation of the impact of climate change on reference crop evapotranspiration in Hamedan-Bahar plain. International Journal of Hydrology Science and Technology 11 (3), 333. doi:10.1504/IJHST.2021.114554.

Tan, M., Zheng, L., 2019. Increase in economic efficiency of water use caused by crop structure adjustment in arid areas. Journal of Environmental Management 230, 386–391. doi:10.1016/j.jenvman.2018.09.060.

Teuling, A.J., de Badts, E.A.G., Jansen, F.A., Fuchs, R., Buitink, J., Hoek van Dijke, A.J., Sterling, S.M., 2019. Climate change, reforestation/afforestation, and urbanization impacts on evapotranspiration and streamflow in Europe. Hydrology and Earth System Sciences 23 (9), 3631–3652. doi:10.5194/hess-23-3631-2019.

Uzhydromet (Center of Hydrometeorological Service of the Republic of Uzbekistan), 2021. Long-term climatic data.

Vanderlinden, K., Giráldez, J.V., Van Meirvenne, M., 2004. Assessing Reference Evapotranspiration by the Hargreaves Method in Southern Spain. Journal of Irrigation and Drainage Engineering 130 (3), 184–191. doi:10.1061/(ASCE)0733-9437(2004)130:3(184).

Vertessy, R.A., Watson, F.G.R., O'Sullivan, S.K., 2001. Factors determining relations between stand age and catchment water balance in mountain ash forests. Forest Ecology and Management 143 (1–3), 13–26. doi:10.1016/S0378-1127(00)00501-6.

Vörösmarty, C.J., Green, P., Salisbury, J., Lammers, R.B., 2000. Global Water Resources: Vulnerability from Climate Change and Population Growth. Science 289 (5477), 284–288. doi:10.1126/science.289.5477.284.

Wang, H., Xiao, W., Zhao, Y., Wang, Y., Hou, B., Zhou, Y., Yang, H., Zhang, X., Cui, H., 2019. The Spatiotemporal Variability of Evapotranspiration and Its Response to Climate Change and Land Use/Land Cover Change in the Three Gorges Reservoir. Water 11 (9), 1739. doi:10.3390/w11091739.

Wang, Q., Cheng, L., Zhang, L., Liu, P., Qin, S., Liu, L., Jing, Z., 2021. Quantifying the impacts of land-cover changes on global evapotranspiration based on the continuous remote sensing observations during 1982–2016. Journal of Hydrology 598, 126231. doi:10.1016/j.jhydrol.2021.126231.

Xu, C., Gong, L., Jiang, T., Chen, D., Singh, V.P., 2006. Analysis of spatial distribution and temporal trend of reference evapotranspiration and pan evaporation in Changjiang (Yangtze River) catchment. Journal of Hydrology 327 (1–2), 81–93. doi:10.1016/j.jhydrol.2005.11.029.

Yang, G., Deng, Y., Lan, P., Xie, L., He, T., Su, X., Shi, X., Chen, G., 2022. Estimation of evapotranspiration in Eucalyptus plantation and mixed forests based on air temperature and humidity. Forest Ecology and Management 504, 119862. doi:10.1016/j.foreco.2021.119862.

Yang, L., Feng, Q., Adamowski, J.F., Alizadeh, M.R., Yin, Z., Wen, X., Zhu, M., 2021. The role of climate change and vegetation greening on the variation of terrestrial evapotranspiration in northwest China's Qilian Mountains. Science of The Total Environment 759, 143532. doi:10.1016/j.scitotenv.2020.143532.

Yang, L., Feng, Q., Yin, Z., Deo, R.C., Wen, X., Si, J., Liu, W., 2020. Regional hydrology heterogeneity and the response to climate and land surface changes in arid alpine basin, northwest China. CATENA 187, 104345. doi:10.1016/j.catena.2019.104345.

Zhang, L., Dawes, W.R., Walker, G.R., 2001. Response of mean annual evapotranspiration to vegetation changes at catchment scale. Water Resources Research 37 (3), 701–708. doi:10.1029/2000WR900325.

Zhang, T., Peng, J., Liang, W., Yang, Y., Liu, Y., 2016. Spatial–temporal patterns of water use efficiency and climate controls in China's Loess Plateau during 2000–2010. Science of The Total Environment 565, 105–122. doi:10.1016/j.scitotenv.2016.04.126.

Zhao, A., Zhu, X., Liu, X., Pan, Y., Zuo, D., 2016. Impacts of land use change and climate variability on green and blue water resources in the Weihe River Basin of northwest China. CATENA 137, 318–327. doi:10.1016/j.catena.2015.09.018.

Zhao, Y., Zou, X., Gao, J., Xu, X., Wang, C., Tang, D., Wang, T., Wu, X., 2015. Quantifying the anthropogenic and climatic contributions to changes in water discharge and sediment load into the sea: A case study of the Yangtze River, China. Science of The Total Environment 536, 803–812. doi:10.1016/j.scitotenv.2015.07.119.

Zhou, D., Hao, L., Kim, J.B., Liu, P., Pan, C., Liu, Y., Sun, G., 2019. Potential impacts of climate change on vegetation dynamics and ecosystem function in a mountain watershed on the Qinghai-Tibet Plateau. Climatic Change 156 (1–2), 31–50. doi:10.1007/s10584-019-02524-4.

Zhou, G., Wei, X., Chen, X., Zhou, P., Liu, X., Xiao, Y., Sun, G., Scott, D.F., Zhou, S., Han, L., Su, Y., 2015. Global pattern for the effect of climate and land cover on water yield. Nature Communications 6 (1), 5918. doi:10.1038/ncomms6918.